

Properties of Spiral Galaxies

The properties of spiral galaxies can be summarized as follows:

- Classically speaking, most spiral galaxies can be de-composed into an elliptical galaxy-like bulge, and an exponential law disk. In other words, in the absence of a bulge, the surface brightness of a spiral galaxy is simply

$$\left(\frac{I}{I_0}\right) = e^{-r/r_d} \quad (7.01)$$

where I_0 is the galaxy's central surface brightness in units of $\text{ergs cm}^{-2} \text{ s}^{-1} \text{ arcsec}^{-2}$ and r_d is the scale length of the exponential. However, not all spiral galaxies have a bulge, and in some galaxies (such as M31), a de-composition into a de Vaucouleur bulge plus an exponential disk does not work very well.

- In the more modern view, spiral galaxies are decomposed into a bulge, a “thin disk” and a “thick disk”. The thick disk may be composed of accreted material, or it may be an older thin disk population that has been “puffed up” by the action of accreted satellite galaxies. Still another view has the thick disk being the simple extension of the bulge population.

- Although the surface brightness of a disk declines exponentially, the e-folding scale length is generally not the scale length you measure in the optical. The amount of internal extinction also declines with radius, effectively flattening the surface brightness distribution of the disk. (The effect is greater in high-inclination galaxies, where your line-of-sight encounters more dust, so the amount of extinction is greatest.)

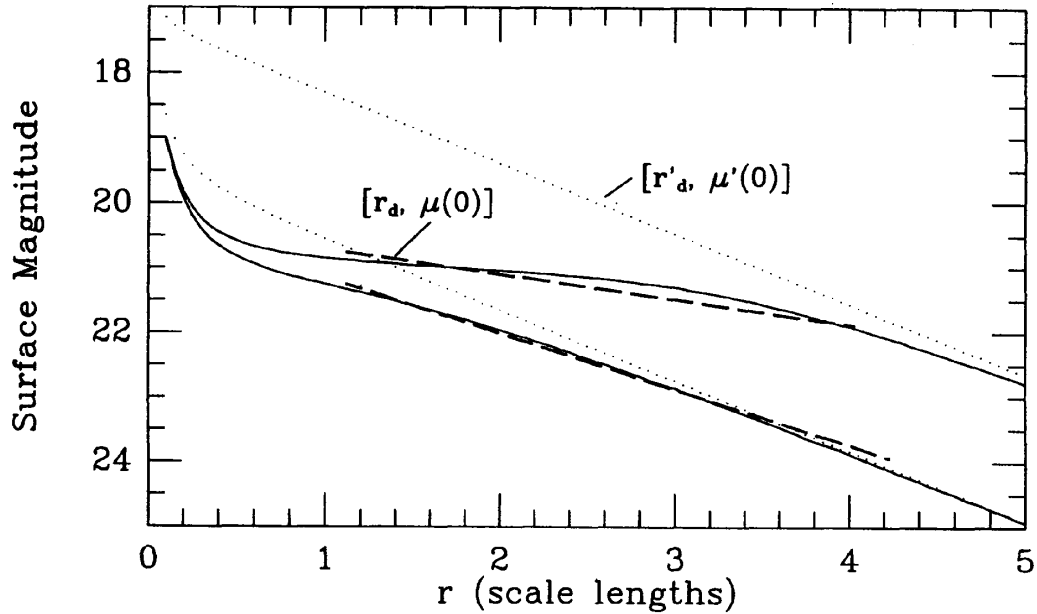


FIG. 4. Dramatization of the effects of absorption on photometric profiles. *Lower solid line*: profile of a low inclination disk, with some absorption in inner parts; *lower dotted line*: unabsorbed, exponential stellar disk with scale length r'_d plus a bulge with 7% of total light; *lower heavy-dash line*: exponential fit to absorbed profile between 1.1 and 4.2 scale lengths r'_d . *Upper solid line*: same galaxy profile seen highly inclined to the line of sight; *upper dotted line*: unabsorbed profile of the inclined disk; *upper heavy-dash line*: exponential fit to absorbed, inclined profile, between 1.1 and $4.0r'_d$, yielding fit parameters $[r_d, \mu(0)]$. Ordinate scale is arbitrary.

[Giovanelli *et al.* 1994, *A.J.*, 107, 2036]

- The exponential law for spiral disks usually continues to four or five scale lengths. After that, disks seems to divide into three types: Type I disks, whose exponential profile extends to the limits of detection (sometimes up to ~ 10 scale lengths), truncated Type II disks, whose exponential profile steepens in the outer regions, and Type III anti-truncated disks, which have a shallower slope at very large galactocentric radii. Minor mergers and interactions may be the cause of this diversity.

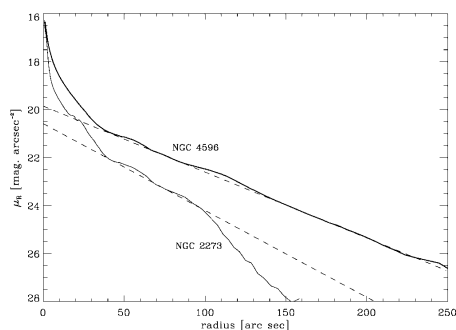


Fig. 1.—Truncated and untruncated surface brightness profiles of barred galaxies; azimuthally averaged surface brightness profiles for NGC 4596 (SB0) and NGC 2273 (SBa), along with exponential fits (*dashed lines*). NGC 4596 shows a type I exponential profile extending to at least 6.3 scale lengths with no sign of truncation; NGC 2273 shows a truncation at $r \sim 3.3$ scale lengths.

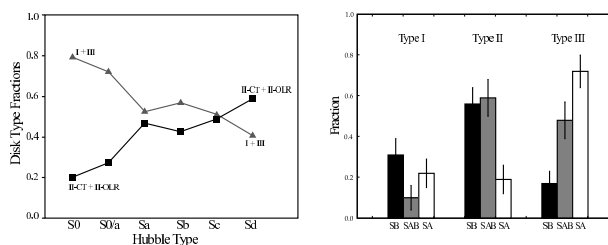


Figure 1. **Left:** General trends of disk-profile type with Hubble type. We separate “truncations” (Type II profiles) from non-truncated profiles (single-exponential Type I and “antitruncated” Type III; see Erwin et al. 2008). Note that the majority of Type II profiles in S0–Sb galaxies are OLR-related, in contrast to the “classical” truncations that dominate late-type spirals. **Right:** The distribution of bar strengths (black = SB, gray = SAB, white = SA) as a function of disk-profile type for early-type (S0–Sb) field galaxies. Type II profiles are clearly more common in barred galaxies, but rare in unbarred galaxies; conversely, Type III profiles (antitruncations) are least common in strongly barred galaxies and most common when there is no bar.

[Erwin *et al.* 2005, *Ap.J.*, **626**, 81]

[Erwin *et al.* 2008, *ASP Conf # 396*, 207]

- The stellar density perpendicular to the disk of a galaxy is often parameterized as an exponential,

$$I(z) \propto e^{-z/z_0} \quad (7.02)$$

where z_0 is the scale height. However, this vertical scale height differs for different types of stars. Below are some rough vertical scale heights for stars in solar neighborhood:

Object	Scale Height (pc)
O stars	50
Cepheids	50
B stars	60
Open Clusters	80
Interstellar Medium	120
A stars	120
F stars	190
Planetary Nebulae	260
G Main Sequence Stars	340
K Main Sequence Stars	350
White Dwarfs	400
RR Lyr Stars	2000

Another often used parameterization is that of an “isothermal” disk. Under this condition, the velocity dispersion (*i.e.*, the distribution of stellar energies) is independent of height above the plane. In such a model, the Jeans equation

$$\frac{\partial}{\partial z} \left\{ \frac{1}{\nu} \frac{\partial}{\partial z} (\nu \langle v_z^2 \rangle) \right\} = -4\pi G \rho \quad (30.66)$$

becomes

$$\frac{\partial}{\partial z} \left\{ \frac{1}{\nu(z)} \frac{\partial \nu(z)}{\partial z} \right\} = -\frac{4\pi m G \nu(z)}{\langle v_z^2 \rangle} \quad (7.03)$$

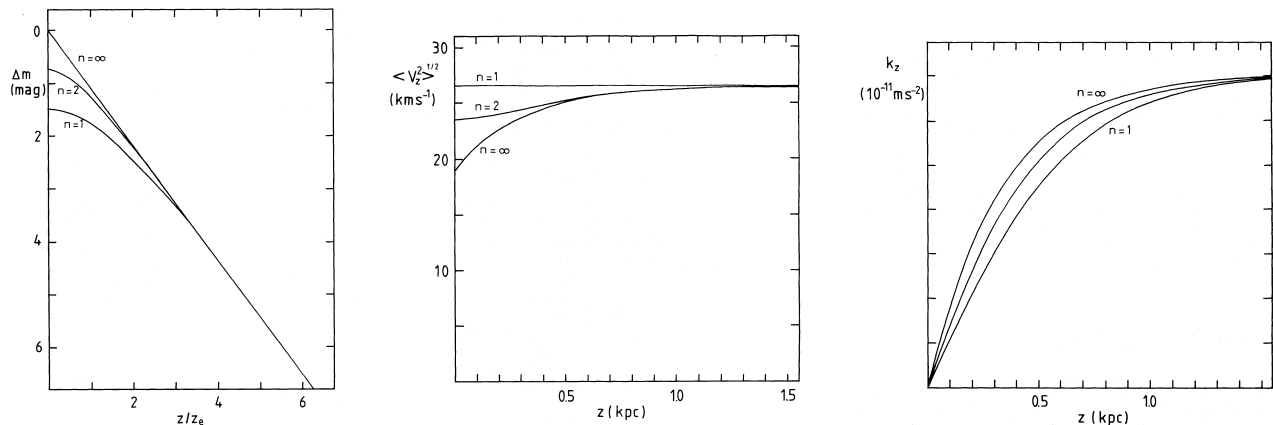
where m is the mass of the stellar particle. The solution to this equation is

$$\rho(z) = \rho_0 \operatorname{sech}^2\left(\frac{z}{2z_0}\right) \quad \text{where} \quad z_0 = \left(\frac{\langle v_z^2 \rangle}{8\pi G \rho_0}\right)^{1/2} \quad (7.04)$$

Note that since

$$\operatorname{sech}(z) = \frac{1}{\cosh(z)} = \frac{2}{e^z + e^{-z}} \quad (7.05)$$

the vertical distribution is very close to exponential except near the midplane. (Also, the derivative of this function is continuous at $z = 0$). Careful observations suggest that the most common disk is actually closer to the intermediate case (between exponential and isothermal), where $\rho \propto \operatorname{sech}(z)$.



Vertical density distribution (left), stellar velocity dispersion (middle), and vertical gravitational force (right) for isothermal ($n = 1$), intermediate ($n = 2$), and exponential ($n = \infty$) disks.

[van der Kruit 1988, *Astr. Ap.*, **192**, 117]

• For a long time, it was thought that the central surface brightness of spiral disks was approximately $B \sim 21.65 \pm 0.3 \text{ mag arcsec}^{-2}$) for all galaxies; this was known as the Freeman law. But, with the advent of CCDs, this was discovered to be a selection effect – it is easier to identify high surface brightness objects than low surface brightness objects. While the central surface brightness of spiral disks is seldom brighter than $B \sim 21.7$, the distribution of fainter central surface brightnesses is roughly flat.

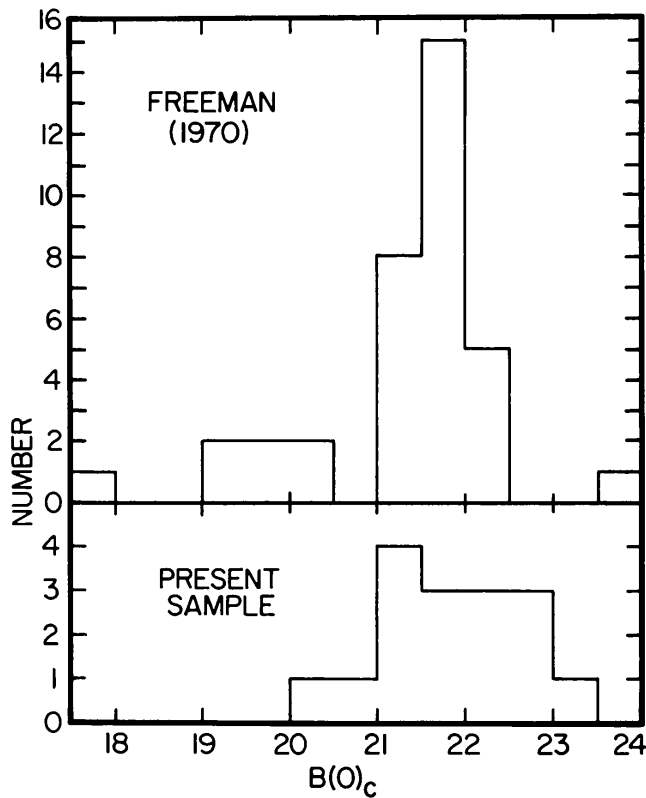


FIG. 7.—The distribution of disk central surface brightness in this study (*lower panel*) and in the study of Freeman (1970) (*upper panel*).

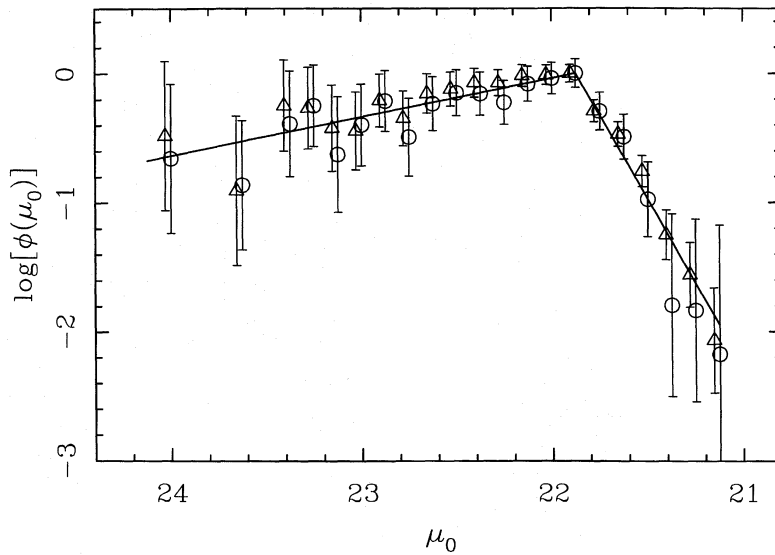


Figure 5. The surface brightness distribution derived from the data of Davies (1990). Circles are data selected by diameter, while triangles are magnitude-limited data. Error bars are from counting statistics. The line is a least-squares fit to the data giving equal weight to points from diameter- and magnitude-limited samples. The distribution declines slowly faintwards of the Freeman value, indicating a large space density of low surface brightness galaxies. It cuts off sharply brightwards of μ_0^* in analogy with the turndown of the luminosity function at L^* .

[Freeman 1970, *Ap.J.*, **160**, 811]

[Borson 1981, *Ap.J. Supp.*, **46**, 177]

[McGaugh 1996, *MNRAS*, **280**, 337]

- Bright spirals are more metal rich than faint spirals. Similarly, early-type (Sa, Sb) spirals are, in general, more metal-rich than equivalent late-type (Sc, Sd) spirals.

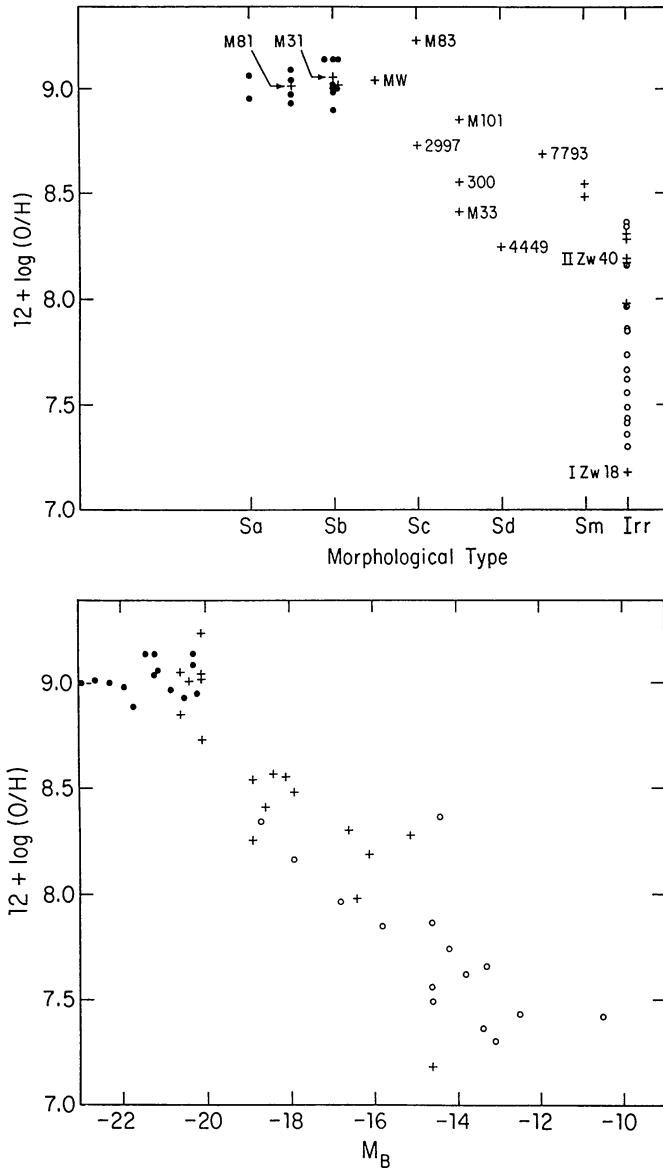


Figure 7 O/H abundance vs morphological type (*upper*) and absolute magnitude (*lower*). Different symbols represent different sources: filled circles—Oey & Kennicutt (1993), plus signs—Garnett & Shields (1987), open circles—Skillman et al (1989). The absolute magnitudes are as given in these references.

[Roberts & Haynes 1994, *ARAA*, **32**, 115]

- Most spirals have radial metallicity gradients. The gradients appear to be shallower in early-type systems, but are still present.

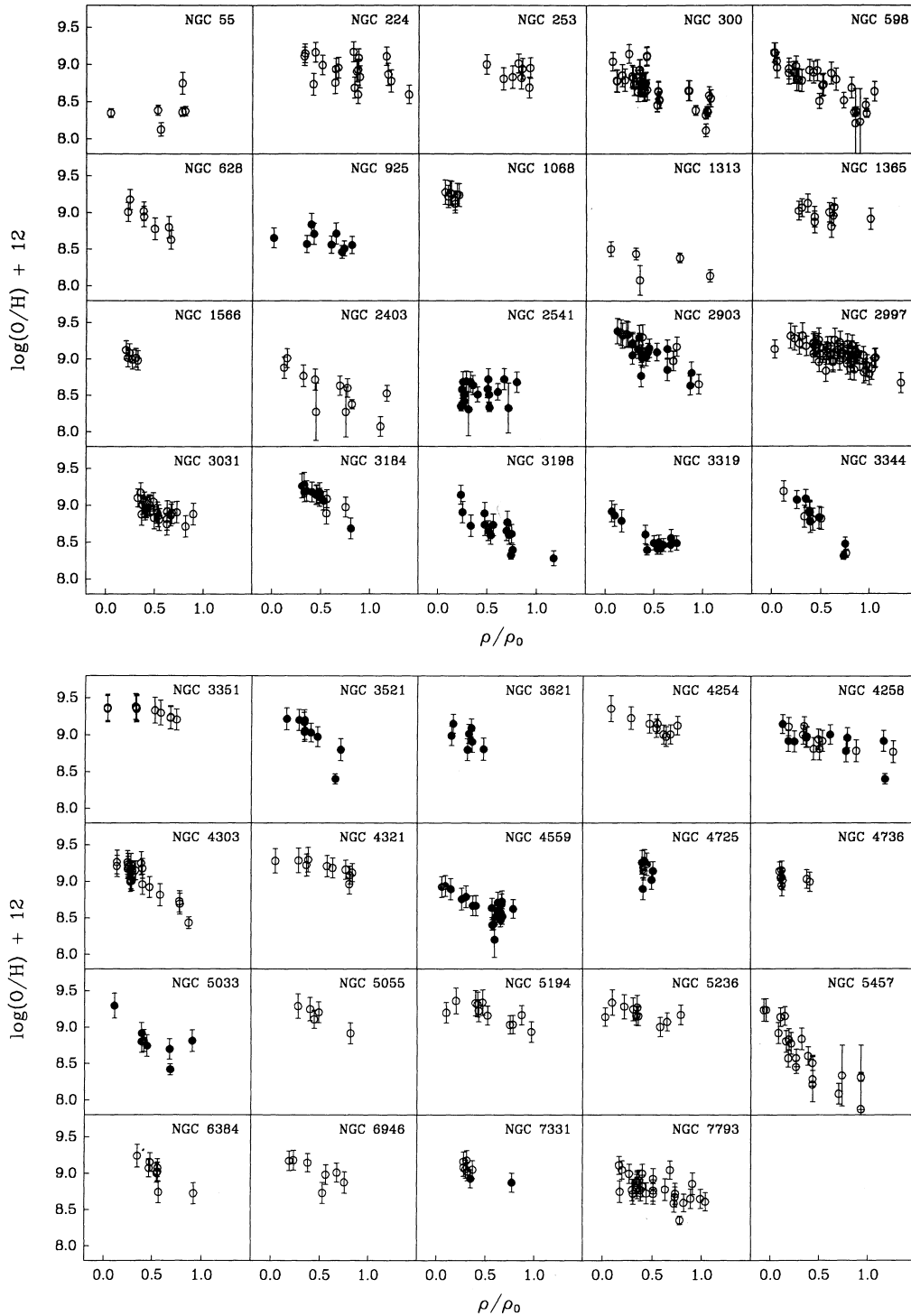


FIG. 8.—Abundances for spiral galaxies with more than five H II regions observed are plotted vs. fractional isophotal radius (\equiv radius/isophotal radius). Our data are presented with filled circles, while that from the literature is presented with open circles.

[Zaritsky *et al.* 1994, *Ap.J.*, 420, 87]

- Spiral galaxies typically have “flat” rotation curves that do not decline with radius. This suggests that the dominant source of matter in the galaxy is in the form of an isothermal halo. To see this, consider that for circular orbits,

$$\frac{GM(r)}{r^2} = \frac{v_c^2}{r} \quad (7.06)$$

Now at large radii, even non-singular isothermal spheres follow an $\rho \propto r^{-2}$ density law. In that case, the mass contained within within a radius R is

$$\mathcal{M}(R) = \int_0^R 4\pi r^2 \rho(r) dr = \int_0^R 4\pi r^2 \frac{\rho_0}{r^2} dr = 4\pi \rho_0 R \quad (7.07)$$

Thus,

$$\frac{G(4\pi\rho_0 R)}{R^2} = \frac{v_c^2}{R} \quad (7.08)$$

or

$$v_c = (4\pi G\rho_0)^{1/2} \quad (7.09)$$

In other words, a rotation law that is independent of radius.

- In the disk of spiral galaxies, there does not appear to be much dark matter. This can be proved from the z motions of stars in the local neighborhood (or in face-on spiral galaxies). If we integrate the isothermal disk density law (7.04) in the z -direction, we obtain

$$\begin{aligned}\Sigma &= \int_{-\infty}^{\infty} \rho(z) dz = 2 \int_0^{\infty} \rho_0 \operatorname{sech}^2 \left(\frac{z}{2z_0} \right) dz \\ &= 2\rho_0 z_0 \tanh \left(\frac{z}{2z_0} \right) \Big|_0^{\infty} = 4\rho_0 z_0\end{aligned}\tag{7.10}$$

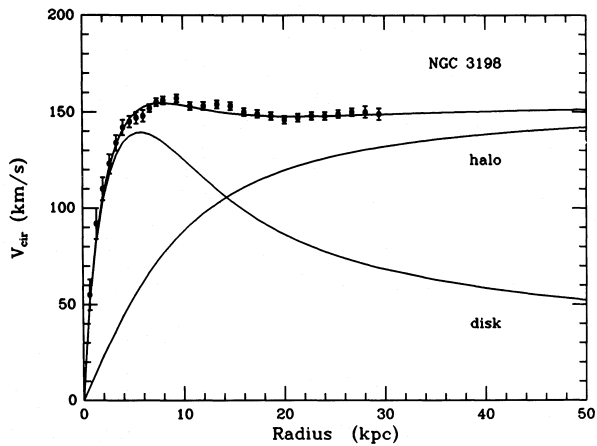
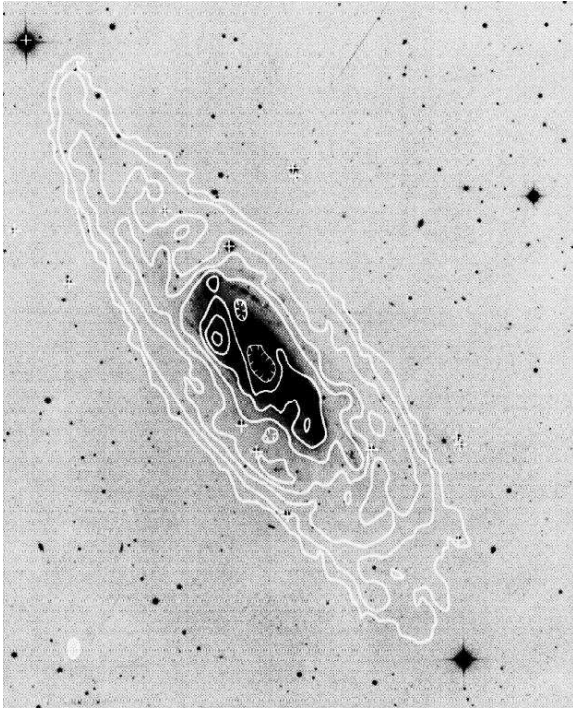
where Σ is the surface density of mass in the disk. When you substitute for ρ_0 using (7.04), this yields

$$\Sigma = \frac{\langle v_z^2 \rangle}{KGz_0}\tag{7.11}$$

where $K = 2\pi$. Since z_0 , the scale height of the isothermal disk, and $\langle v_z^2 \rangle$, the velocity dispersion of stars in the direction perpendicular to the disk, are both measurable, the disk mass can be measured independent of the rotation curve. The results are consistent with the local census of stars and interstellar matter, with no need for dark matter.

Note that, in the more general case of non-isothermal disks, the result is similar, though the constant K changes. ($K = \pi$ for an exponential disk, $K = \pi^2/2$ for the intermediate case; see van der Kruit 1988 for this derivation.)

- At small radii, baryonic disk mass dominates in spiral galaxies. At the galactic radius increases, the disk mass declines, but the dark halo mass increases just enough to keep the rotation curve flat. This is sometimes called the “disk-halo conspiracy.”



[van Albada *et al.* 1985, *Ap.J.*, **295**, 305]

- There is a tight relation ($< 20\%$) between a spiral galaxy's rotation rate and its total luminosity. For circular orbits,

$$\frac{GMm}{r^2} = \frac{mv_c^2}{r} \implies \frac{M}{r} \propto v_c^2 \quad (7.12)$$

The luminosity-line width (or Tully-Fisher relation) says that

$$\mathcal{L} \propto v^a \quad (7.13)$$

where a depends on the bandpass of the observations. (For the B -band, $a \sim 2.9$, but for the infrared (where internal extinction is unimportant), the exponent is ~ 3.5 . Obviously, the two equations put together imply that

$$\mathcal{L} \propto \left(\frac{\mathcal{M}}{r} \right)^{a/2} \quad (7.14)$$

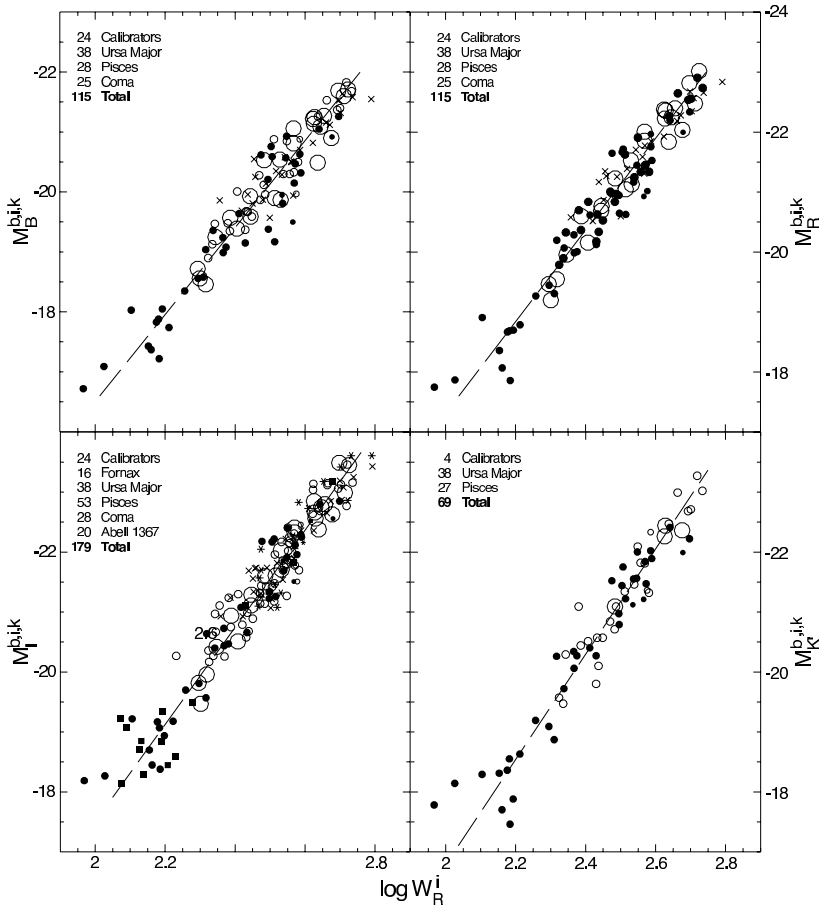


FIG. 6.— B , R , I , and K' absolute magnitude-line width relations for the cluster template galaxies translated to overlay on the zero-point calibrator galaxies. Symbols and straight line fits as in previous plots. The I relation involves five clusters and 24 zero-point calibrators, the B and R relations are built with three clusters and 24 zero-point calibrators, and the K' relation is based on two clusters and four zero-point calibrators. Relative distances between clusters and with respect to the calibrators are the same on all plots.

[Tully & Pierce 2000, *Ap. J.*, **533**, 744]

Rotation Curves for Exponential Disks

[Binney & Tremaine 1987, *Galactic Dynamics*]

Often, as a reflex, we write down the potential of a system with enclosed mass $\mathcal{M}(r)$ as relate it to circular velocity as

$$\Phi(r) = \frac{G\mathcal{M}(r)}{r} = v_c^2 \quad (7.15)$$

But in general, this is not true. Take the potential of an exponential disk. In the plane of a thin disk with scale length r_d and central surface mass Σ_0 , the potential is

$$\Phi(R, 0) = -\pi G \Sigma_0 r [I_0(y)K_1(y) - I_1(y)K_0(y)] \quad (7.16)$$

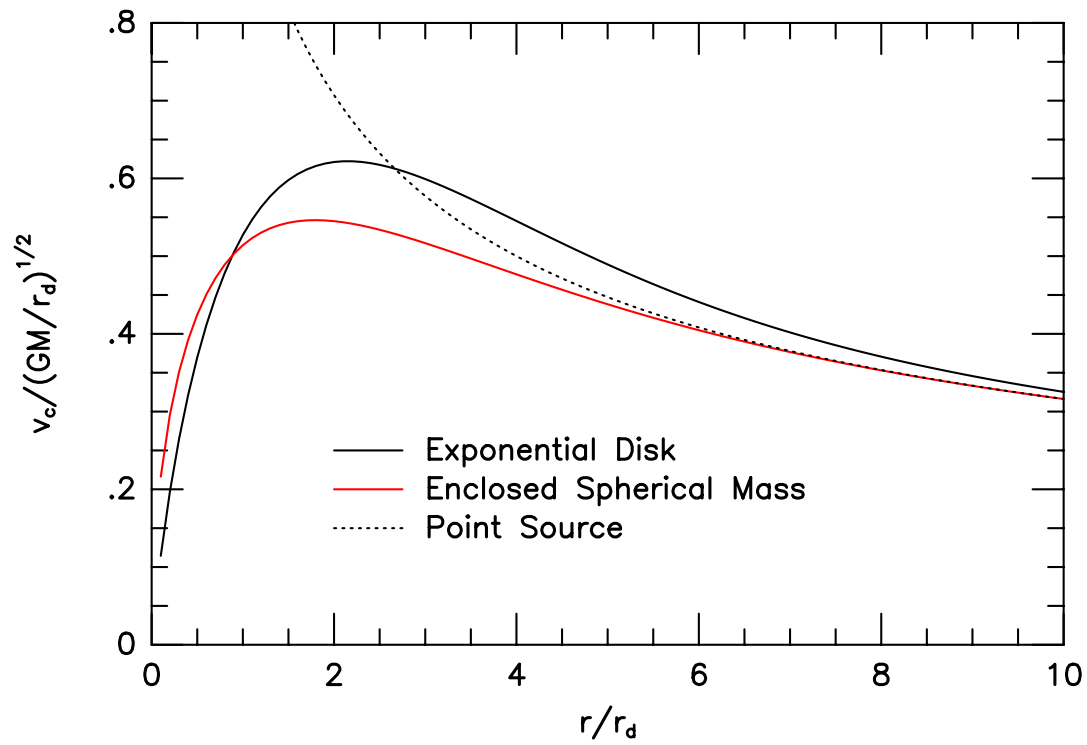
where $y = r/(2r_d)$, and I_n and K_n are modified Bessel functions of the first and second kinds. (You can find out all about these functions in Abramowitz & Stegun, and most mathematical packages, including *Numerical Recipes*, has subroutines to evaluate them.) The rotation curve at any radius is then given by

$$v_c^2(r) = r \frac{d\Phi}{dr} \quad (7.17)$$

which, for the exponential disk, is

$$v_c^2 = 4\pi G \Sigma_0 r_d y^2 [I_0(y)K_0(y) - I_1(y)K_1(y)] \quad (7.18)$$

As the plot below shows, this is different from what you would get with a spherical distribution of mass.



Properties of Dwarf Galaxies

[Mateo 1998, *A.R.A.A.*, **36**, 435]

Dwarf galaxies have very different properties from either spiral or elliptical galaxies. Normally, dwarf galaxies are defined as objects with absolute B magnitudes fainter than -16 . There are three types of dwarf galaxies: dwarf ellipticals (dE), dwarf spheroidals (dSph), and dwarf irregulars (dI). Unfortunately, astronomers are *very* sloppy in their terminology, so it is sometimes hard to understand which type is being talked about.

Dwarf Ellipticals are the low luminosity extension of normal giant elliptical galaxies; they obey the same relation as their larger counterparts. An example of a dwarf elliptical is M32. (Actually, M32 is more compact than a normal elliptical, since it has been tidally stripped of its outer stars by M31.)

Dwarf Spheroidals are gas-poor, diffuse systems whose density profile is closer to an exponential disk than an $r^{1/4}$ law. These objects do not fall on the elliptical galaxy fundamental plane, and, in the Morgan classification scheme, would be given the letter “D” instead of “E”. Examples are NGC 147 and the Leo I dwarf.

Dwarf Irregulars are low-luminosity extensions to spiral galaxies. In general, these objects are brighter than the dSph galaxies since they have active star formation, but if their star formation were to cease, they might evolve into a dSph. The Small Magellanic Cloud is a dwarf irregular.

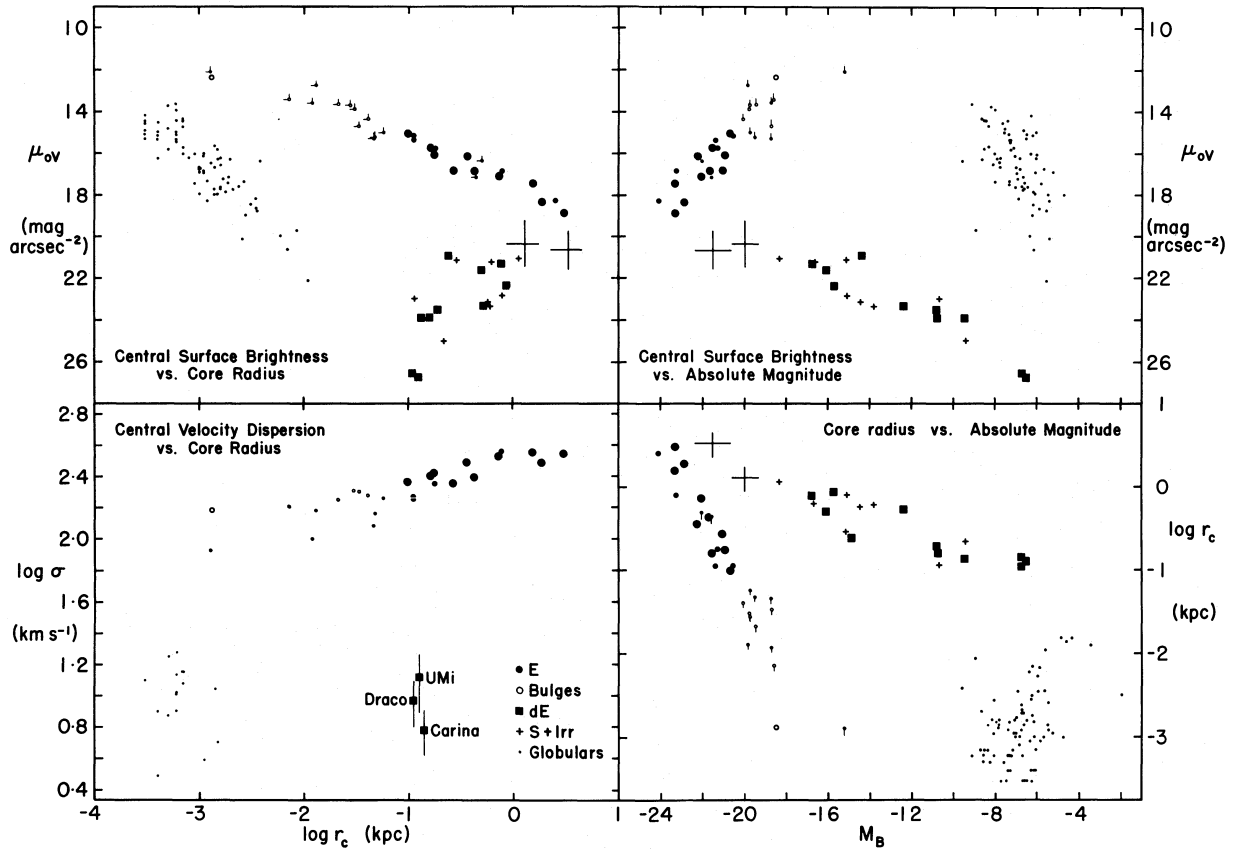
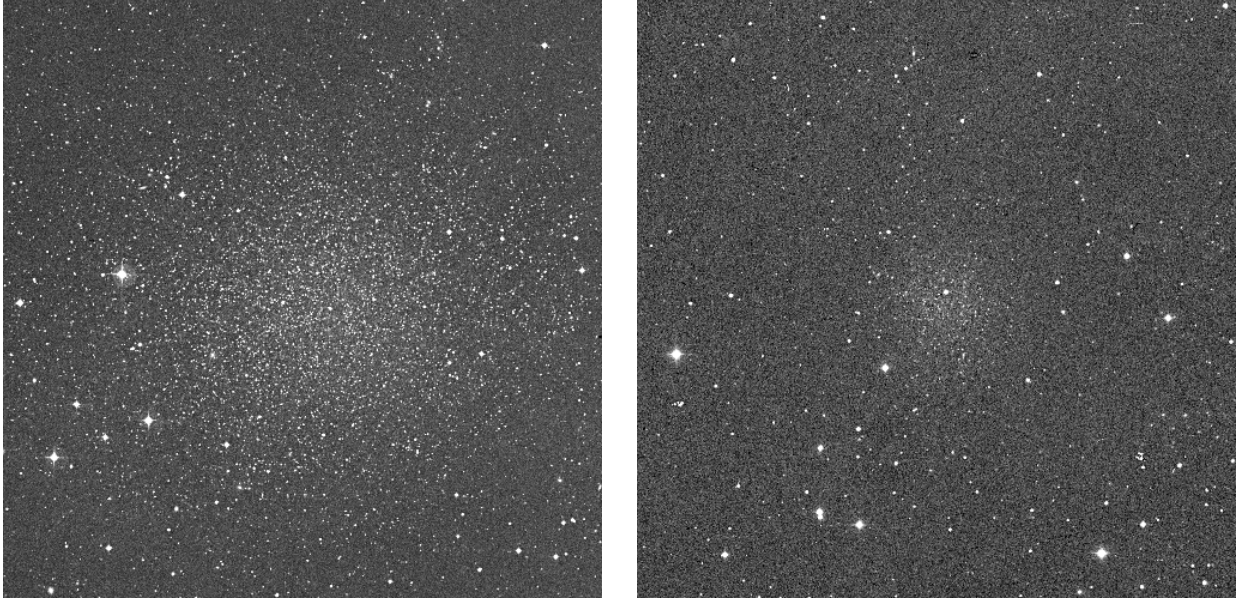


FIG. 3.—Comparison of the core parameter relations for various kinds of stellar systems. Bulges and ellipticals are as in Fig. 2. The dwarf elliptical galaxies are, in order of decreasing luminosity, IC 3349, 12^h52, and 13^h66 (Virgo Cluster designations from Binggeli, Sandage, and Tarenghi 1984), NGC 147, Fornax, Leo I, Sculptor, Leo II, Draco, Carina, and UMi. Similarly, the dS + Irr galaxies are the generic large disk (two points), LMC, SMC, NGC 6822, WLM, IC 1613, Sextans A, GR 8, and LGS-3. The discrepant globular cluster at upper left ($\mu_{0V} = 16.38$ mag arcsec⁻², $\log r_c = -2.42$) is, of course, ω Cen.

[Kormendy 1985 *Ap. J.*, 295, 73]

Dwarf galaxies have the following properties:

- Dwarf galaxies are typically very metal poor (but not as metal-poor as a Pop II globular cluster). This is consistent with the general mass-metallicity relationship that seems to hold for all galaxies.

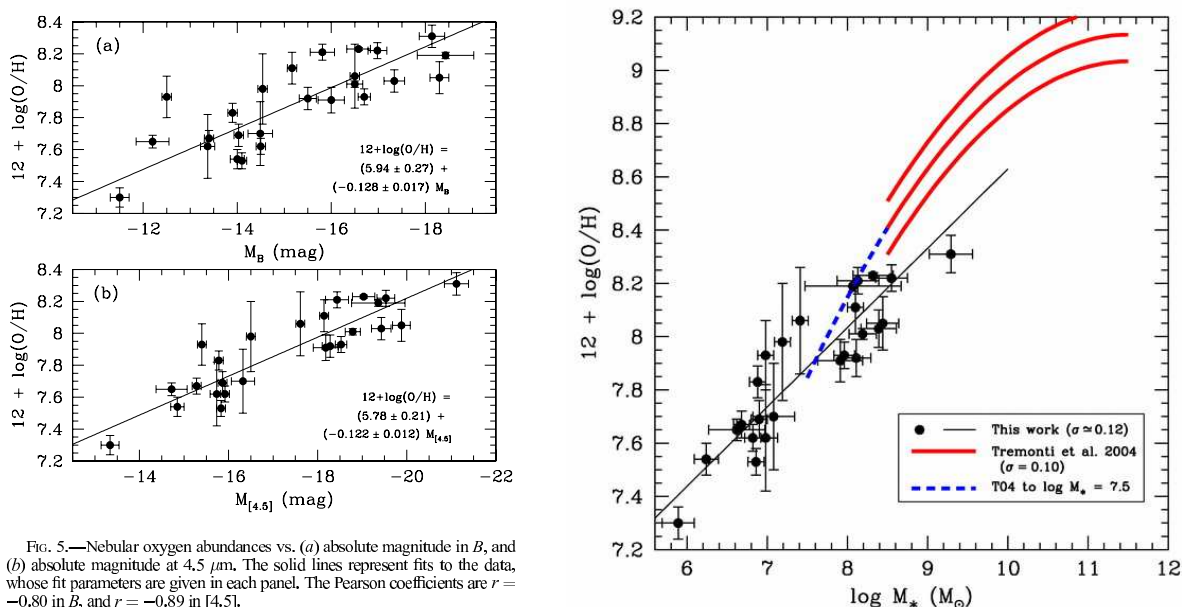
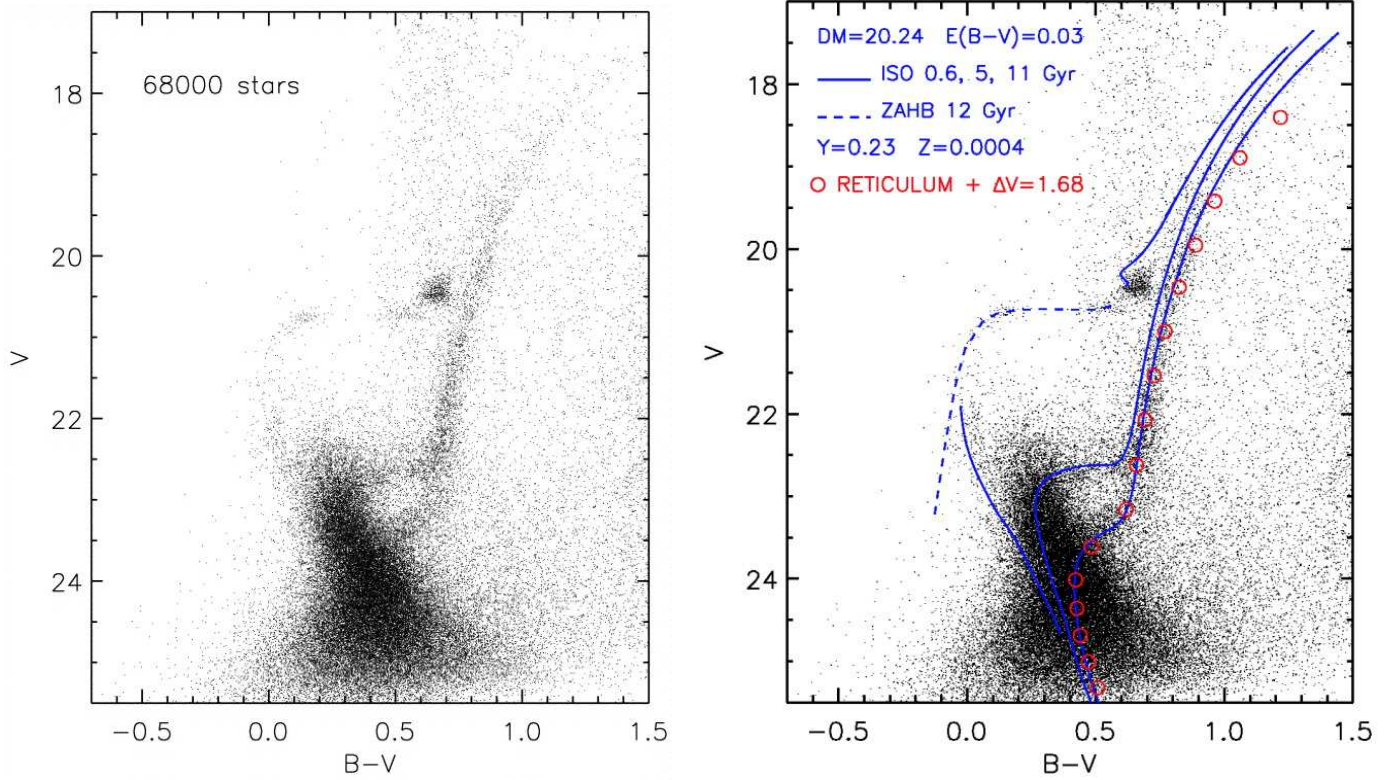


Fig. 5.—Nebular oxygen abundances vs. (a) absolute magnitude in B , and (b) absolute magnitude at $4.5 \mu\text{m}$. The solid lines represent fits to the data, whose fit parameters are given in each panel. The Pearson coefficients are $r = -0.80$ in B , and $r = -0.89$ in $[4.5]$.

[Lee *et al.* 2006, *Ap.J.*, **647**, 970]

- Dwarf galaxies show evidence for more than one burst of star formation. (As we'll see, this is a very curious feature.)



[Monelli *et al.* 2003 *A.J.*, **126**, 218]

- Dwarf galaxies can be “nucleated.” Their nuclei are sometimes interpreted as being a small bulge.
- The mass-to-light ratio of dwarf spheroidals (as found from individual stellar kinematics) can be extremely large! The smaller the dwarf galaxy, the larger its apparent mass-to-light ratio.

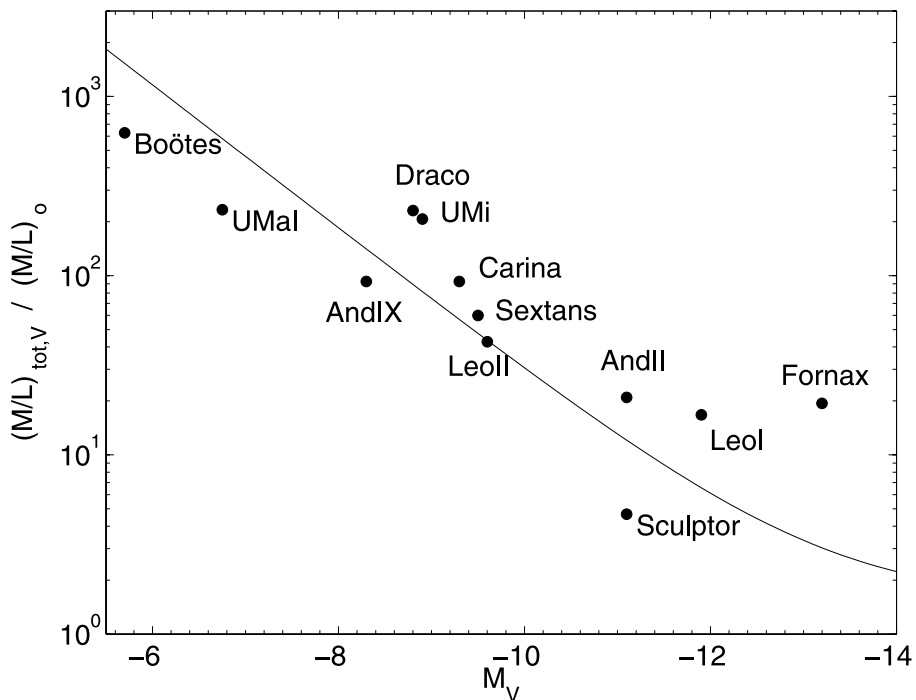


FIG. 5.—Updated Mateo plot. Mass-to-light ratios are plotted vs. absolute magnitudes for Local Group dwarf galaxies, following a style suggested by Mateo et al. (1993) and Mateo (1998, his Fig. 9, *bottom panel*). The solid line is the relation for a constant mass (dark) halo. The modern data shown here extend the original relation by three magnitudes in luminosity and an order of magnitude in mass-to-light ratio, while reducing the scatter by an order of magnitude. Data are from the tables in the text, except for And II (Côté et al. 1999) and And IX (Chapman et al. 2005). Values for Sculptor, And II, And IX, UMa I, and Boötes are based on small kinematic samples and are less certain than are the results for the other galaxies. We explain this correlation as a consequence of the characteristic minimum galaxy scale size shown in Fig. 1 convolved with the narrow range of mass profiles and mean dark matter densities shown in Fig. 4.

[Gilmore *et al.* 2007 *Ap.J.*, **663**, 948]

- Unlike high-surface brightness galaxies, where baryons dominate in the central regions, dwarf spheroidals and other low surface-brightness galaxies should be dark matter dominated, throughout. Thus, by measuring their rotation curves, we should be able to probe the dark matter distribution at all radii.

CDM and Λ CDM models all predict that galaxies have “dark matter cusps”, *i.e.*, the density of dark matter should increase rapidly near the galactic center. This prediction is typified by the N -body simulations of Navarro, Frenk, & White (1996), who found that, in terms of the critical density of the universe, dark halos today have the generic density profile

$$\frac{\rho(r)}{\rho_{\text{crit}}} = \frac{\delta_c}{(r/r_s)(1 + r/r_s)^2} \quad (7.18)$$

where δ_c is the halo’s (dimensionless) overdensity, and r_s , the characteristic radius of the halo, is defined as the galaxy’s virial radius (r_{200}) divided by a dimensionless concentration (c). In the NFW formulation, every dark matter halo is defined by two parameters, the concentration, and the virial radius, r_{200} : the mass of the halo is given by

$$\mathcal{M}_{200} = 200 \rho_{\text{crit}} \left(\frac{4\pi}{3} \right) r_{200}^3 \quad (7.19)$$

and the overdensity, δ_c , is set by the concentration

$$\delta_c = \frac{200}{3} \frac{c^3}{[\ln(1 + c) - c/(1 + c)]} \quad (7.20)$$

From this, the circular velocity (*i.e.*, the rotation curve) arising from the dark matter alone should be given by

$$\left[\frac{v_c(r)}{v_{200}} \right]^2 = \frac{1}{x} \frac{\ln(1 + cx) - (cx)/(1 + cx)}{\ln(1 + c) - c/(1 + c)} \quad (7.21)$$

where $x = r/r_{200}$ and

$$v_{200} = \left(\frac{GM_{200}}{r_{200}} \right)^{1/2} \quad (7.22)$$

This law fits the rotation curves of spirals and explains the dynamics of binary galaxies extremely well. However, it does *not* agree with the results from low surface brightness galaxies. These objects have much less dark matter in their cores than predicted by CDM models.

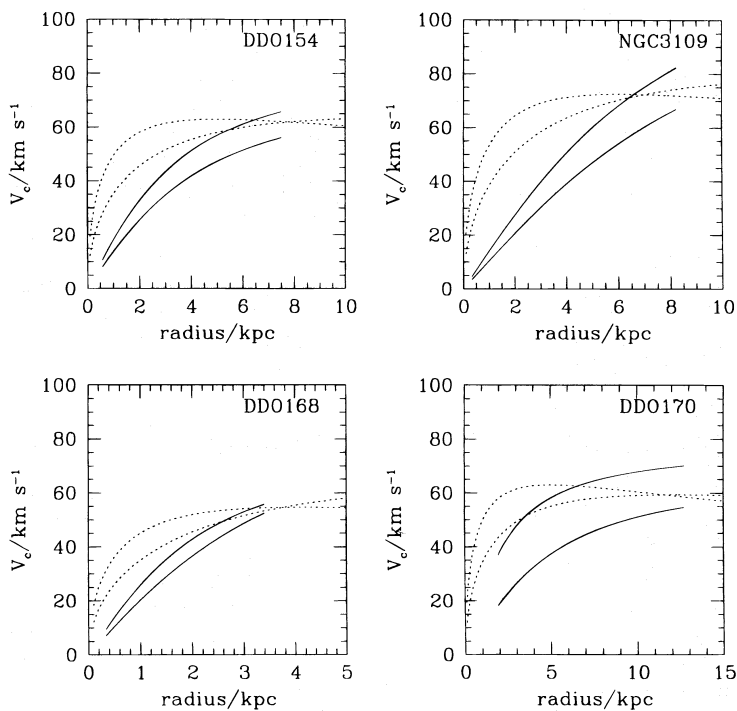


FIG. 12.—Circular velocities of CDM halos (*dotted lines*) compared with the halo contribution to the rotation curve of four dwarf galaxies (*solid lines*). The solid lines encompass the likely contribution of the halo and correspond to the “maximal” and “minimal” disk hypotheses. CDM halos seem to be significantly more concentrated than allowed by observations.

[Navarro, Frenk, & White 1996, *Ap.J.*, **462**, 563]